PHYSICAL REVIEW D **74,** 033004 (2006)

What can we learn from neutrino electron scattering?

André de Gouvêa and James Jenkins

Department of Physics & Astronomy, Northwestern University, 2145 Sheridan Road, Evanston, Illinois 60208, USA

(Received 12 April 2006; published 7 August 2006)

Precision tests of the standard model are essential for constraining models of new physics. Neutrino-electron elastic scattering offers a clean probe into many electroweak effects that are complimentary to the more canonical measurements done at collider facilities. Such reactions are rare, even as compared with the already tiny cross sections for neutrino-nucleon scattering, and competitive precision measurements have historically been challenging to obtain. Because of new existing and proposed high-flux neutrino sources, this is about to change. We present a topical survey of precision measurements that can be done with neutrino-electron scattering in light of these new developments. Specifically, we consider four distinct neutrino sources: nuclear reactors, neutrino factories, beta beams, and conventional beams. For each source we estimate the expected future precision of several representative observables, including the weak mixing angle, neutrino magnetic moments, and potential leptonic Z' couplings. We find that future neutrino-electron scattering experiments should add nontrivially to our understanding of fundamental physics.

DOI: 10.1103/PhysRevD.74.033004 PACS numbers: 13.15.+g, 12.15.−y, 12.38.Qk, 13.85.Dz

I. INTRODUCTION

Neutrino-electron scattering offers a clean probe into the standard model of particle physics as well as many of its extensions. ''Clean'' refers to the fact that this process is very well understood theoretically. There are no hadronic complications, so that the underlying electroweak physics (including potential deviations from standard model expectations) is directly accessible. It is therefore ''easy'' to use such reactions to test the consistency of the standard model (SM), determine precision electroweak parameters, and look for signatures of new physics. When this is considered along with the large variety of natural and artificial sources that yield high-flux neutrino samples of multiple flavors over a vast energy range, it seems that neutrino-electron scattering provides an ideal laboratory for electroweak studies.

This line of reasoning appears misleading when realistic considerations are made. While theoretically ideal, the study of neutrino-electron scattering is experimentally challenging due to its tiny cross section, which forces one to pursue very intense sources and large targets. More serious is the fact that the neutrino-nucleon scattering cross section is generally 3 orders of magnitude larger and serves as a large potential source of background. Naively, one may consider simply subtracting off such background statistically. In this case, the uncertainty induced by the subtraction is approximately $\sqrt{10^3} \approx 30$ times larger than the intrinsic statistical uncertainty of the signal; clearly unacceptable for precision measurements. Of course, this is a worst-case scenario: experimental setups usually allow one to isolate the signal events by performing various ''cuts'' on the data. Exactly how this is done depends on the energy and flavor of the incident neutrino beam, as well as on the details of the detector.

The signal we concentrate on is a single forward electron with no other detector activity, and all detectors considered can distinguish, with varying degrees of success, electrons from various potential background sources. Cuts on event timing, rate of energy loss in the detector, and threshold energy, to name a few, aid in this endeavor (details are discussed in Sec. II B). Even with optimistic particle identification abilities, experiments must still account for irreducible backgrounds. This is particularly relevant in ν_e and $\bar{\nu}_e$ sources, where the charged current neutrino-nucleon reaction $\nu_e N \to eX$ can yield a final state that is often consistent with a single recoil electron. Such backgrounds, however, can still be reduced by exploiting additional constraints. For example, electrons produced by neutrino-electron scattering are constrained by kinematics to have small transverse momenta $p_t \propto \sqrt{m_e}$, whereas the electron p_t distribution in most background events is much broader, $p_t \propto \sqrt{m_{\text{nucleon}}}$. Therefore, an experiment with good p_t resolution can significantly constrain this class of background events. After all available data analyzing resources are spent, one is (hopefully) left with a signal-dominated event sample. This being the case, the remaining beam-related background can be modeled and subtracted, inducing a (much smaller) statistical uncertainty on the final data sample. Backgrounds related to other neutrino/radiation sources originating from extraterrestrial, terrestrial, and artificial origins are typically controlled by introducing shielding and imposing clever p_t, timing, and energy cuts. The resulting backgrounds and uncertainties will typically be small, and are therefore not considered here. Finally, one must also account for other experimental systematic uncertainties in the final analysis, which may or may not dominate the sensitivity budget.

These considerations imply that measurements of neutrino-electron elastic scattering can be limited mainly by statistics and uncertainties related to the neutrino source. In order to accumulate enough statistics, one is required to commit to long running experiments with large

detectors close to the neutrino source; a practice that has proven fruitful in the recent past, but not sufficient to yield results competitive with other tests of electroweak physics. Significant progress is expected to be made with the advent of improvements to the neutrino sources themselves, both in statistics and flux normalization.

Currently existing sources that could be used for neutrino-elastic scattering purposes can be broadly classified as either reactors or conventional neutrino beams, and are both discussed in Sec. II B. These are still subject to some of the limitations described above, which, in some cases, prevent competitive electroweak "precision" measurements. Recent progress in the development of two new classes of neutrino beams inspires the possibility of sidestepping these limitations and thereby testing the SM to unparalleled accuracy. Neutrino factories and β-beams offer high luminosity neutrino beams with well-known energy spectra [1]. Here, we explore the potential of neutrino-electron scattering experiments in light of our enhanced knowledge of these sources.

The paper is organized in the following manner. Section II reviews the relevant tree-level SM cross sections, making brief mention of first order electroweak corrections. We then describe the various neutrino sources—reactors, conventional beams, β-beams, and ν-factories—used in our analysis. In each case we describe the energy spectrum, as well as uncertainties and backgrounds relevant to their associated neutrino-electron scattering experiments. Section III begins with a short description of our analysis, after which we review and motivate various observables and present our results on projected sensitivities to each within the context of future scattering experiments. Specifically, we discuss measurements of the weak mixing angle θ_W, neutrino electromagnetic moments μ_ν, neutrino neutral current left-handed couplings ρ, and potential leptonic Z' couplings. We conclude in Sec. IV with a summary of our results and an outlook for the future.

II. FORMALISM

We are interested in "elastic" neutrino-electron and antineutrino-electron scattering, characterized by $\nu_\ell e^- \to \nu_{\ell'} e^-$, where ℓ, $\ell' = e$, μ, τ, and ν stands for either a neutrino or an antineutrino state. Note that, given our inability to identify the neutrino flavor after it has scattered off the target electron, there is no way of recognizing whether the scattered neutrino has the same lepton-flavor number or lepton number as the incoming one.

The basis of this analysis is the differential event spectrum $dN(T)/dT$. This is the number of neutrino-electron elastic scattering events within the interval T to $T + dT$ of electron recoil kinetic energy. It involves the convolution of the differential cross section $d\sigma(T, E_\nu)/dT$ and the incoming neutrino energy spectrum, $d\Phi(E_\nu)/dE_\nu$. More than one neutrino flavor/helicity may be produced at each of the sources listed in Sec. II B and, since the final state electrons scattered from the various neutrino types are experimentally indistinguishable, their contributions must be incoherently added, leading to

$$\frac{dN(T)}{dT} = (\text{time}) \times (\#\ \text{targets}) \times \sum_i^{\text{flavors}} \int dE_\nu \frac{d\Phi_i(E_\nu)}{dE_\nu} \frac{d\sigma_i(T, E_\nu)}{dT}, \quad (2.1)$$

where (# targets) is the total number of target electrons in the detector and (time) is the time duration of the experiment. In order to use Eq. (2.1), we must know the flux and the cross sections, along with their associated uncertainties. These are reviewed in the following subsections. For the remainder of this work, unless stated otherwise, we assume a 100 ton detector of similar capabilities as Minerva [2], located 100 m from the neutrino source, running for one year.[1]

A. Cross sections

In the standard model (SM), all tree-level differential cross sections for neutrino-electron scattering can be expressed as

$$\frac{d\sigma}{dT}(\nu_\ell e \to \nu_\ell e) = \frac{2G_\mu^2 m_e}{\pi E_\nu^2}[a^2 E_\nu^2 + b^2(E_\nu - T)^2 - abm_e T], \quad (2.2)$$

where G_μ is the Fermi constant, E_ν is the energy of the incident neutrino, and T is the kinetic energy of the recoil electron. a and b are process-dependent constants that, within the SM, depend on the weak mixing angle θ_W, as tabulated in Table I. The cross term proportional to m_e, the mass of the electron, is relevant for low energy applications, but is negligible in processes where $E_\nu \gg m_e$.

Since the incident neutrinos are all produced by some charged current process, we assume that all incoming neutrinos (antineutrinos) are strictly left handed (right handed). Given our understanding of the charged current interactions, this is an excellent approximation even if one considers the existence of exotic helicity-flipping processes whose amplitudes are necessarily proportional to the neutrino mass, and therefore negligible for all practical purposes. We further assume that all electron targets are unpolarized.

For $\ell = \mu$, τ, the scattering process proceeds via t-channel Z-boson exchange. The $\nu_e e \to \nu_e e$ and $\bar{\nu}_e e \to \bar{\nu}_e e$ reactions proceed via a combination of t-channel Z-boson, and t/s-channel W-boson exchange, respectively, and are related by $a \leftrightarrow b$ exchange. In Sec. III D, we will discuss the sensitivity of neutrino-electron scattering to the left-handed neutrino coupling to the Z-boson, referred to as

[1]One year is defined to be 3.16×10^7 s.

TABLE I. Standard model a and b parameter values for the differential cross section, given by Eq. (2.2). Here $s^2 \equiv \sin^2\theta_W \approx 0.231\,49 \pm 0.000\,15$ [3], where θ_W is the electroweak mixing angle, and $\ell = \mu, \tau$.

	$\nu_e e \to \nu_e e$	$\bar{\nu}_e e \to \bar{\nu}_e e$	$\nu_\ell e \to \nu_\ell e$	$\bar{\nu}_\ell e \to \bar{\nu}_\ell e$
a	$-\frac{1}{2} - s^2$	$-s^2$	$\frac{1}{2} - s^2$	$-s^2$
b	$-s^2$	$-\frac{1}{2} - s^2$	$-s^2$	$\frac{1}{2} - s^2$

ρ. In the SM, $\rho = 1$ at tree level. For arbitrary values of ρ, the cross section for $\nu_\ell e^-$ scattering simply scales with ρ^2 in the $\ell = \mu, \tau$ case, while the dependency is more involved in the $\ell = e$ case. We return to this issue in Sec. III D.

Current experimental precision allows the extraction of many electroweak observables to better than 1%, introducing the need to go beyond the simple tree-level cross sections outlined above. Indeed, neutrino-electron scattering experiments must include full first (and perhaps second) order corrections into their analysis to maintain consistency [4]. These corrections are theoretically well known, and can be easily applied to data analysis [5,6]. See [7] for a pedagogical review of calculations involving electroweak radiative corrections. Here we briefly summarize the results of such first order effects, utilizing the minimal subtraction ($\overline{\text{MS}}$) renormalization scheme. See [4,8] for the full expressions.

The full $\mathcal{O}(\alpha)$ corrections to the νe cross sections given by Eq. (2.2) involve one-loop effects as well as photon bremsstrahlung. QED effects (in the relevant high energy limit) are well described by a T and E_ν dependent, $\mathcal{O}(\alpha)$ modification of the a, b parameters:

$$a^2(\text{or } b^2) \to a^2(\text{or } b^2)[1 + \alpha F_{a(b)}(T, E_\nu)], \qquad (2.3)$$

where F_a and F_b are dimensionless functions of T and E_ν. The remaining corrections are generally q^2 dependent and parametrized by the running of the weak mixing angle $\sin^2\theta_W$, and the deviation of ρ from its tree-level value of 1. These relations depend weakly on the Higgs mass, which we take to be 150 GeV. The net result is an approximately 1% shift in the total integrated cross section.

Given the precision with which next-generation experiments can probe the physics of neutrino-electron scattering, higher order corrections, while small, are by no means irrelevant, and need to be taken into account. We would like to emphasize, however, that the effect of higher order SM corrections is negligible *for the purposes of this paper*. This is a consequence of the fact that we are interested in gauging the *precision* (δo, o for observable) of various measurements, not in computing what their central values ($\bar{o}$ for the extracted value) are. Generally, $\frac{\delta o}{\bar{o}} \approx$ few % for the observables of interest, thus the dependence on electroweak corrections $\delta_{EW}(\frac{\delta o}{\bar{o}}) \approx (1\%)^2 = 0.01\%$ can be ignored. That being said, our analysis does in fact incorporate first order SM effects. However, in the spirit of simplicity, we shall refrain from mentioning them and always refer to the tree-level cross sections of Eq. (2.2) when necessary.

B. Fluxes

In our analysis, the specific details of the incoming neutrino energy spectrum matter little for determining an experiment's sensitivity to an observable. How well we know that spectrum is, however, of the utmost importance, as is the overall luminosity, mean beam energy, and neutrino flavor composition. The sample sources used in our analysis were chosen to span a large range of possible configurations. Specifically, we consider four types of neutrino sources yielding distinct flavor content and energy spectra over a broad energy range. These are nuclear reactors, neutrino factories, β-beams, and conventional beams. Their respective energy spectra are depicted in Fig. 1. Note that there are other potential experimental setups capable of precision neutrino-electron scattering [9]. These will not be considered in this study.

1. Reactor

Nuclear reactors are intense sources of low energy (< 10 MeV) $\bar{\nu}_e$'s, and continue to play a central role in neutrino physics [10]. The nuclear fuel in a modern light water reactor is typically enriched with (2–5)% ^{235}U and produces 3 GW of thermal power. On average, 200 MeV and 6 neutrinos are released with each fission, thus yielding around $5 \times 10^{20} \bar{\nu}_e$/s [10]. The main limitation of a reactor as a source of antineutrinos is that the fissions occur at rest, implying isotropic emission: you cannot "focus" the reactor beam.

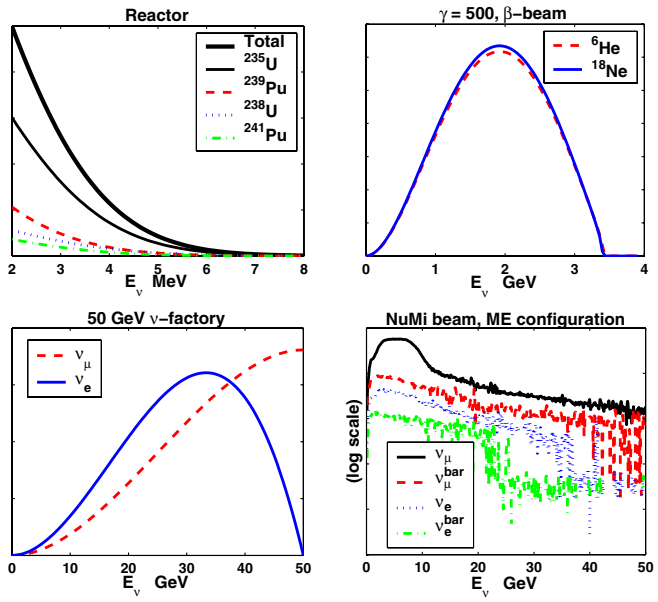

FIG. 1 (color online). Neutrino energy spectra for different neutrino sources. Flux normalizations are arbitrary.

While it is relatively simple to predict the absolute magnitude of emitted neutrinos, predicting their energy spectra requires detailed modeling. In an actual neutrino experiment, the thermal power of the reactor[2] is measured as a function of time. With this and the initial fuel composition, the fission rate can be modeled for the dominant isotopes. These are ^{235}U, ^{239}Pu, ^{238}U, and ^{241}Pu, and they typically fission, in an average fuel cycle, by the proportions 25:10:4:3. Other isotopes such as ^{240}Pu and ^{242}Pu contribute to the flux at the $\mathcal{O}(0.1\%)$ level and can be safely neglected. Combined with knowledge of the induced decay of these dominant isotopes by thermal neutrons, this procedure predicts the reactor $\bar{\nu}_e$ energy spectrum to better than 10% and the total flux to nearly 1% [11]. Here, we will employ an empirical relation to describe the neutrino flux [12,13].[3]

$$\frac{d\Phi_{\bar{\nu}_e}(E_\nu)}{dE_\nu} = N\sum_i n_i e^{a_{0i}+a_{1i}E+a_{2i}E^2}, \tag{2.4}$$

where i runs over the dominant parent fission isotopes ^{235}U, ^{239}Pu, ^{238}U, and ^{241}Pu and the n_i's are related by the proportions mentioned above. Table II lists the coefficients of the exponentiated polynomial in Eq. (2.4) for each isotope [14], as well as the relative n values [10]. The top-left panel of Fig. 1 depicts them individually along with the total $\bar{\nu}_e$ flux. The absolute normalization N is found from the requirement that the total neutrino rate be 2×10^{20} (power/GW) s^{-1}.

At these energies, the inverse β-decay process

$$\bar{\nu}_e p \rightarrow e^+ n \tag{2.5}$$

is the dominant source of background by a factor greater than 100. Because of its threshold of 1.8 MeV, only about 25% of the released neutrinos will trigger such a reaction. This begs the question of why neutrino scattering experiments are done with the high energy >2 MeV tail of the spectrum, in the presence of lower statistics and a significant source of background. Some experiments do, in fact, use low energy reactor neutrinos; they are primarily designed to search for neutrino magnetic moments or study neutrino-nucleus coherent scattering [15]. The difficulty in working within this energy range is the uncertainty in the neutrino flux, which can be as large as 30% [11]. Flux measurements have not been made below ≈ 2 MeV and theoretical calculations are not reliable due to an increase in the number of β-decay chains with low Q^2 values, many of which are not completely understood. To complicate matters further, long-lived isotopes, residing in spent fuel stored on-site, radiate in this range and must be tracked and accounted for in a reliable analysis.

TABLE II. Coefficients of the exponentiated second order polynomial in the reactor antineutrino flux Eq. (2.4), adapted from [14]. Average n_i values were extracted from [10].

i	a_{0i}	a_{1i} MeV^{-1}	a_{2i} MeV^{-2}	n_i
^{235}U	0.904	−0.184	−0.0878	25
^{239}Pu	1.162	−0.392	−0.0790	10
^{238}U	0.976	−0.162	−0.0790	4
^{241}Pu	0.852	−0.126	−0.1037	3

In the (2–8) MeV region, a detector capable of distinguishing the inverse β-decay reaction from the signal with high efficiency is needed. A study of the uncertainties associated with reactor neutrinos as relevant to neutrino-electron scattering at these energies was presented in [16]. There, the authors assume a 26.5 ton CHOOZ-like detector [17] composed of oil scintillator located ~225 m from two 3.6 GW nuclear reactors. Such an experiment is optimized for $\bar{\nu}_e p \rightarrow e^+ n$ detection, but can also be used to identify and reconstruct the energy of the final state electron in $\bar{\nu}_e e \rightarrow \bar{\nu}_e e$. In general, these two processes are distinguished by the detection of the final state neutron in Eq. (2.5) via its capture on H and Gd nuclei after a characteristic time in which the neutron thermalizes. This procedure induces some systematic uncertainty on background subtraction from the failure to identify some neutrons within the characteristic time window, resulting in the misidentification of some background as signal. Additionally, other sources of uncertainty arising from experimental factors such as energy calibration and efficiencies must also be included for a realistic analysis. Throughout this work, we refer to these simply as systematic effects and treat them as we do the background subtraction uncertainty. Backgrounds unrelated to the source are controlled by shielding and comparing the on/off reactor states needed for refueling. Following [16], the total uncertainty from background can be minimized to the 1% level by utilizing various experimental cuts. Of particular relevance to our analysis, a cut on the electron visible energy $3\ \text{MeV} < T < 5\ \text{MeV}$ must be applied to achieve such precision. Additionally, by normalizing to the inverse β-decay sample, an uncertainty of order 0.1% can be achieved in the overall neutrino flux normalization [16], an order of magnitude better than that achieved from reactor modeling alone.

Future reactor experiments designed to operate in our selected energy window are optimized to search for the elusive neutrino mixing angle θ_{13} [18] (see Table I of [19]

[2]Other reactor quantities such as water pressure/temperature must be measured and used in the modeling of the neutrino spectrum. These affect the spectrum weakly. See [10] for more details.

[3]The chemical composition of the fuel in the reactor also varies as a function of time, and must be considered in order to translate reactor flux measurements into physics observables. The impact of this time evolution is, however, negligible when it comes to estimating the precision with which physics observables can be measured. Therefore, for the purposes of the upcoming analysis, it suffices to deal with the average fuel compositions.

for a concise list of future experiments along with many of their projected specifications such as reactor power, detector baselines, and fiducial mass). All of the proposed facilities include at least one near detector at around 100 m from the source to help control the various source-related systematic uncertainties. Such sites can serve as ideal next-generation laboratories for the study of low energy neutrino-electron scattering. Of these, the Double CHOOZ experiment [20] should be the first to begin taking data, and could significantly help explore many of the topics surveyed here.

For our analysis we assume a single 3 GW reactor, with a flux given by Eq. (2.4) known to 0.1%. Furthermore, we apply the visible energy cut $3\ \mathrm{MeV} < T < 5\ \mathrm{MeV}$ described above, along with an induced 1% systematic uncertainty arising from background subtraction. With this in place, an experiment running for one year should record approximately 10^4 signal events, which implies a 1% statistical uncertainty.

2. Neutrino factory

The concept of a neutrino factory has received much attention in recent years and is now entering a serious development stage [1]. The concept is simple: produce and isolate a copious amount of muons from an intense (> 1 MW) proton beam incident on a fixed target. Boost them to the desired energy and then inject them into a storage ring with a long straight section. The boosted muons in the straight section will decay in flight into two neutrinos nearly 100% of the time [3]:

$$\mu^- \rightarrow e^- \nu_\mu \bar{\nu}_e, \tag{2.6}$$

$$\mu^+ \rightarrow e^+ \bar{\nu}_\mu \nu_e. \tag{2.7}$$

Neutrinos that result from muon decay in straight sections are beamed in the forward direction by an amount dependent on the boost factor γ of the parent muon. The specific flavor composition of the resulting collimated neutrino beam is a simple consequence of the sign of the selected parent muon. Clearly, the beam will consist of equal proportions of muon-type and electron-type neutrinos, where one is a particle and the other an antiparticle. The geometry of the storage ring can be optimized so that a maximum percentage of muons decay in the straight section (approximately 35%).

In the muon's rest frame, the decays Eq. (2.6) and (2.7) are described by the following well-known expressions [1]:

$$\frac{d^2\Phi_{\nu_\mu}}{dE_\nu d\Omega_{cm}} \propto \frac{4E_\nu^2}{\pi m_\mu^4}(3m_\mu - 4E_\nu), \tag{2.8}$$

$$\frac{d^2\Phi_{\nu_e}}{dE_\nu d\Omega_{cm}} \propto \frac{24E_\nu^2}{\pi m_\mu^4}(m_\mu - 2E_\nu), \tag{2.9}$$

where E_ν refers to the energy of the emitted neutrino in the muon's rest frame. Equations (2.8) and (2.9) are valid for both μ^+ and μ^- decays, provided that the muon beam has zero net polarization. For a polarized beam, an additional term is generated that changes sign under $\mu^+ \leftrightarrow \mu^-$. This possibility is not considered here, but can easily be introduced and is not expected to affect any of our results (we refer readers to [1] and references therein for the status and implications of polarized muon beams as applied to a neutrino factory).

Given Eqs. (2.8) and (2.9), it is straightforward to obtain the electron-type and muon-type neutrino fluxes at any boosted reference frame. The bottom-left panel of Fig. 1 shows the on-axis energy spectra of a 50 GeV neutrino factory beam. Both the ν_μ and ν_e beam components are shown without distinguishing between neutrino and antineutrino because they yield the same spectrum. The absolute normalization is obtained by requiring that the integrated flux over solid angle and energy yields 10^{20} decays/year [21]. Neutrino factory designs aim at reaching a 0.1% uncertainty on the flux normalization [22]. This can be further reduced by half from normalizing to the muon regeneration process $\nu_\mu e \rightarrow \mu^- \nu_e$ and $\bar{\nu}_e e \rightarrow \mu^- \bar{\nu}_\mu$. A neutrino factory running in the μ^- mode of Eq. (2.7) is subject to a very real source of background via the inverse beta-decay reaction, which must be reduced by applying p_t cuts. A beam running in the μ^+ mode is not affected by this, but still may be subject to other background events that contain a single final state electromagnetic shower that mimics the electron signal, such as coherent and diffractive π^0 production. These must be dealt with during data analysis. After all expected analysis cuts, the resulting signal-to-background ratio is projected to be better than five [22]. Under such high statistics conditions, backgrounds are negligible when compared to the overall flux-normalization uncertainty and additional systematic effects.

For our analysis, we assume 10^{20} muon decays per year in the straight section of the storage ring producing a neutrino flux given by the boosted version of Eqs. (2.8) and (2.9). The uncertainty on the absolute normalization is taken to be 0.1% and 0.05% for μ^+ and μ^- beams, respectively, with negligible induced statistical uncertainty arising from background subtraction. Additional systematic uncertainties in such neutrino factory experiments are difficult to estimate and may be large as compared to the values listed here. We therefore perform our analysis assuming a systematic uncertainty ranging from (0–5)%. With this, an experiment running for one year with a 50 GeV beam should record approximately 10^9 elastic scattering events, inducing a statistical uncertainty of only 0.003%.

3. β-beam

β-beams are newly envisioned facilities that will produce an intense beam of electron-type neutrinos (ν_e or $\bar{\nu}_e$)

with well-known energy spectra. These beams are virtually free of contamination by other neutrino flavors. The idea behind a β-beam is very similar to that of a neutrino factory [1]. β-decaying isotopes are produced by an optimized fixed target collision. They are then accelerated and placed in a storage ring where they undergo β-decay, producing a collimated neutrino beam. Current isotopes of interest are ^{18}Ne for ν_e production and ^{6}He for $\bar{\nu}_e$ production. Approximately 10^{18} decays per year are expected at a β-beam facility for either nuclei, assuming the existing design [23], 35% of which should occur in the straight section of the storage ring and therefore constitute the beam.

β-decay kinematics are well known and lead to the following approximate form for the neutrino energy spectrum in the ion's rest frame:

$$\frac{d^2\Phi}{dE_\nu d\Omega_{cm}} \propto E_\nu^2(E_0 - E_\nu)\sqrt{(E_0 - E_\nu)^2 - m_e^2}, \quad (2.10)$$

where E_0 is the electron end-point energy; 3.5 MeV for ^{6}He and 3.4 MeV for ^{18}Ne. Hence,

$$\left.\frac{d^2\Phi}{dE_\nu d\Omega_{\rm lab}}\right|_{\theta_{\rm lab}\approx 0} \propto \gamma^2 E_\nu^2(E_m - E_\nu) \times \sqrt{(E_m - E_\nu)^2 - (2\gamma m_e)^2}, \quad (2.11)$$

where $E_\nu = 2\gamma E_\nu^{cm}$ is now the transformed energy in the boosted frame and $E_m = 2\gamma E_0$ is the maximum neutrino energy. The top-right panel of Fig. 1 shows the shape of the β-beam flux given by Eq. (2.11) for both isotopes mentioned above and a boost factor $\gamma = 500$, assuming the same overall normalization for each. The small difference between the curves is due to the differences in the β-decay end-point energy. Once again the normalization is found by conditions on the integrated flux and is assumed, as in the neutrino factory case, to be known to approximately 0.1%. The proposed boost factors range from $\gamma = 60$ with a mean energy of 0.2 GeV to $\gamma = 2500$ with a mean energy of 7 GeV. At these energies, the primary source of background is quasielastic scattering (deep inelastic processes become dominant at the high energy facilities). The number of such events can be reduced by imposing kinematical cuts on p_t.

For our analysis, we assume a $\gamma = 500$ β-beam source consisting of 1.1×10^{18} and 2.9×10^{18} decays per year at facilities running in the ν_e (^{18}Ne) and $\bar{\nu}_e$ (^{6}He) modes respectively [23], with an energy spectrum given by Eq. (2.11) carrying an overall 0.1% uncertainty. Although the signal-to-background ratio for such β-beam experiments should be large enough to neglect the statistical uncertainty induced from background subtraction, additional systematic uncertainties may still be large as compared with the other characteristic uncertainties of the system. We therefore perform our analysis assuming systematic uncertainties ranging from (0–5)%. Under these conditions, an experiment running for one year should record 6×10^5 elastic scattering events inducing a statistical uncertainty of only 0.13%.

4. Conventional beams

We define a *conventional beam* broadly as any neutrino source arising primarily from the decay of accelerator-produced pions or kaons. There are currently several conventional neutrino beams in operation or in the development stage. Many were constructed for the primary purpose of studying long/medium baseline neutrino oscillations, but can also be used to study neutrino-electron scattering. A detector, as described here, placed close to the neutrino source would yield a high neutrino-electron statistics sample. This would lead not only to an enhancement of our knowledge of fundamental particle properties, but would serve as a source of normalization for the oscillation experiments as well as reduce uncertainties on cross sections needed to extract oscillation parameters. One example is the K2K beam line, originating from the KEK accelerator facility in Japan which yields a high luminosity broadband ν_μ beam peaking in the sub-GeV energy range to the Super-Kamiokande detector 250 km away [24,25]. A more powerful beam at the currently under construction J-PARC facility is being planned [25]. In the U.S.A., Fermilab is currently home to two important conventional neutrino beams. The booster neutrino beam line provides a low energy (0.5–1.5) GeV, ν_μ beam to the MiniBooNE experiment and may, in the future, also serve the proposed FINeSSE (Fermilab Intense Neutrino Scattering Scintillator Experiment) experiment with an overall flux uncertainty of approximately 5% [26]. At much higher energies, the NuMI (Neutrinos at the Main Injector) beam is planned to power the Minerva [2] detector, which is to be located behind the MINOS near detector. The NuMI beam can operate in different configurations ranging in peak energy from (3–15) GeV. Additionally, it has the option of running in the ''negative'' mode, dominated by ν_μ, or the reverse ''positive'' mode, dominated by $\bar{\nu}_\mu$. Planned upgrades to the Fermilab proton accelerator would significantly enhance the performance of the NuMI beam as it applies to both neutrino oscillation and scattering experiments [27].

Generally, conventional beams consist of ν_μ, $\bar{\nu}_\mu$, ν_e, and $\bar{\nu}_e$, at least to some degree. Muon-type neutrinos are always the most prominent beam component and, of these, the dominant helicity state can be chosen by selecting the sign of the decaying mesons. The bottom-right panel of Fig. 1 shows a log plot of the energy spectrum of the NuMI beam in its medium energy (ME) configuration [28]. In this case, ν_μ is the dominant beam component with $\bar{\nu}_\mu$ contributing at the 3% level and ν_e making up less than 1%. We take the NuMI beam in its medium energy, ν_μ dominated, configuration (shown in the bottom-right panel of Fig. 1) as a representative example throughout this study.

TABLE III. Results on the precision of parameter extraction, assuming a 100 ton detector located 100 m from the neutrino source. All limits are taken at 68% confidence. The bounds in parentheses are computed assuming a worst-case scenario of 5% systematic uncertainty induced from background subtraction. See text for details.

	Assumptions	Uncertainties % background, % flux	$\sin^2\theta_W$ %	Magnetic moment 68%	Z' coupling ϵ 68%	ρ %
Reactor	3 GW, $3 < T < 5$ MeV [16]	1, 0.1	0.82	$4.8 \times 10^{-10}\mu_B$	2.0×10^{-3}	1.1
μ^+ ν-factory	50 GeV, $10^{20}\frac{\text{decays}}{\text{year}}$ [22]	0(5), 0.1	0.14 (6.64)	$2.5(10.1) \times 10^{-11}\mu_B$	$6.9(13.1) \times 10^{-4}$	0.09 (1.2)
μ^- ν-factory	50 GeV, $10^{20}\frac{\text{decays}}{\text{year}}$ [22]	0(5), 0.05	0.04 (8.62)	$3.1(12.4) \times 10^{-11}\mu_B$	$3.3(8.7) \times 10^{-4}$	0.06 (0.93)
β-beam ν_e (^{18}Ne)	$\gamma = 500$, $1.1 \times 10^{18}\frac{\text{decays}}{\text{year}}$ [1]	0(5), 0.1	0.34 (7.60)	$3.0(6.6) \times 10^{-10}\mu_B$	$9.8(16.3) \times 10^{-4}$	0.369 (2.4)
β-beam $\bar{\nu}_e$ (^{6}He)	$\gamma = 500$, $2.9 \times 10^{18}\frac{\text{decays}}{\text{year}}$ [1]	0(5), 0.1	0.22 (5.72)	$2.6(6.7) \times 10^{-10}\mu_B$	$7.7(14.2) \times 10^{-4}$	0.75 (3.1)
Conventional	NuMI on-axis 3.7×10^{20} POT	0(5), 3	0.48 (9.92)	$1.8(6.6) \times 10^{-10}\mu_B$	$2.7(6.4) \times 10^{-3}$	3.3 (7.3)

Optimistically consistent with the above projections, we assume a 3% overall uncertainty on the total flux normalization. Similar to the neutrino factory case, the main sources of background are those events consisting of single electromagnetic showers (with electronlike topologies) which can generally be removed to a negligible level by cutting on their broad p_t distribution. Assuming 3.7×10^{20} protons on target (POT) and the given detector configuration, we expect nearly 10^7 elastic scattering events, inducing a statistical uncertainty of 0.03%.

III. RESULTS

We perform χ^2 analysis to extract the sensitivity of neutrino-electron elastic scattering experiments to $\sin^2\theta_W$, μ_ν, ρ, and potential leptonic Z'-induced couplings ϵ. Table III lists the results of our analysis, along with the key assumptions regarding the different experimental setups. Each result assumes a one year run with a 100 ton fiducial mass detector located 100 m from the neutrino source. We take $\sin^2\theta_W(M_Z)_{\overline{\text{MS}}} = 0.231\,20 \pm 0.000\,15$ at the Z-pole for all our analysis, except when we explore the ability of the different setups to measure the weak mixing angle itself. We also fix $\rho = 1$ (at the tree level) for all our analysis, except when we explore the ability of different setups to measure ρ itself.

A. $\sin^2\theta_W$

The weak mixing angle θ_W parametrizes the change of basis from the $SU(2)_L$ and $U(1)_Y$ gauge fields to the mass eigenfields, the $W^\pm$-boson, the Z-boson, and the photon, after electroweak symmetry breaking. Within the SM, electroweak processes, including those of Eq. (2.2), can be expressed in terms of $\sin^2\theta_W$, G_μ, and the fine-structure constant. It is essential to precisely measure these quantities and check for consistency between the various classes of processes. The current best fit value is $\sin^2\theta_W(M_Z)_{\overline{\text{MS}}} = 0.231\,20 \pm 0.000\,15$ [3], or $\delta(\sin^2\theta_W)/\sin^2\theta_W = 0.065\%$.

The NuTeV collaboration—which studied deep inelastic neutrino-nucleus scattering—extracted a value for $\sin^2\theta_W$ measured at center-of-mass energies near the 50 GeV scale, with $\delta(\sin^2\theta_W)/\sin^2\theta_W = 0.70\%$ precision, that was approximately 3 standard deviations above the SM prediction [29]. Many possible explanations of this discrepancy have been proposed [30], but additional precision measurements must be made to help pinpoint the true culprit, be it new physics or some subtle systematic effect. In particular, neutrino-electron scattering experiments, utilizing the sources described in Sec. II B, should be especially helpful in this endeavor, as they may be subject to the same new phenomena responsible for the NuTeV result, without hadronic complications. It is in this spirit that we summarize the existing (and proposed) measurements of the weak mixing angle via neutrino-electron scattering and present our results.

The most precise ($\delta\sin^2\theta_W/\sin^2\theta_W = 0.069\%$) measurements of the weak mixing angle were done at e^+e^- colliders operating near the Z-pole and dominated by the LEP and SLD experiments [31]. Compared with such precision measurements, the past contribution from neutrino-electron elastic scattering from conventional beam sources at the GeV scale is quite feeble[4] at $\delta\sin^2\theta_W/\sin^2\theta_W = 3.5\%$ [3] resulting mainly from data taken with the CHARM-II detector at the CERN SPS [32], and to a lesser degree from the E734 experiment at the Brookhaven National Laboratory [33]. Both experiments, performed with conventional beams, analyzed the ratio $R = \sigma(\nu_\mu e)/\sigma(\bar{\nu}_\mu e)$ in order to exploit the cancellation of common systematic uncertainties. They therefore took advantage of the ability to run their respective beams in neutrino/antineutrino mode at will, a method that we do not explore in our analysis.

Our results on the weak mixing angle are as follows: At a future reactor experiment, one should be able to measure $\sin^2\theta_W$ with a 0.82% uncertainty at the MeV scale, a result consistent with an estimate made, under similar assump-

[4]Although measurements of the weak mixing angle are much less precise at neutrino-electron scattering experiments, their contributions are still very important. The variability of the various neutrino beam energies helps to demonstrate the running of $\sin^2\theta_W$. Additionally, such processes aid in the search for new physics by signaling inconsistencies with the Z-pole results.

tions, in [16]. A neutrino factory experiment, running in either μ^+ or μ^- mode, can do much better in the absence of systematic uncertainties. Assuming 0% (5%) systematic uncertainty $\delta(\sin^2\theta_W)/\sin^2\theta_W$ at the multi-GeV scale could reach 0.14% (6.64%) and 0.04% (8.62%) at a μ^+ and μ^- 50 GeV neutrino factory, respectively. These results are consistent with the estimates of [22] (which assume a smaller detector situated slightly closer to the source). Measurements of $\sin^2\theta_W$ at low energy ($\gamma < 20$) β-beam sources have recently been discussed in [34] as a function of the expectations for the systematic uncertainties and the number of different combined boost factors γ used in the analysis. They conclude that a 10% measurement of $\sin^2\theta_W$ at low q^2 is within reach of a future β-beam facility, provided systematic uncertainties are held below 10%. Our analysis assumes a much higher energy ($\gamma = 500$) beam, which implies larger statistics. Assuming 0% (5%) systematic uncertainties $\delta(\sin^2\theta_W)$ should reach 0.34% (7.60%) and 0.22% (5.72%) at a ν_e and $\bar{\nu}_e$ β-beam, respectively, near the GeV scale. Finally, at existing or planned conventional neutrino beams, the weak mixing angle could also be measured. Using the NuMI beam, we find that $\sin^2\theta_W$ at a multi-GeV scale can be measured with 0.48% (9.92%) precision, assuming 0% (5%) systematic uncertainty.

B. Neutrino magnetic moments

Neutrino masses imply that neutrinos necessarily have nonzero electromagnetic dipole moments. The nature of μ_ν will depend on whether the neutrinos are Majorana or Dirac fermions and, without loss of generality, these are described by (after electroweak symmetry breaking)

$$\begin{aligned} \mathcal{L} &= \mu_\nu^{ij}(\nu_i \sigma_{\mu\nu} \nu_j F^{\mu\nu}) + \text{H.c. (Majorana)}, \\ \text{or} \quad \mathcal{L} &= \mu_\nu^{ij}(\bar{\nu}_i \sigma_{\mu\nu} \nu_j F^{\mu\nu}) + \text{H.c. (Dirac)}, \end{aligned} \tag{3.1}$$

where $F^{\mu\nu}$ is the electromagnetic field strength. μ_ν^{ij} is, in general, complex, and hence carries information concerning the neutrino electric and magnetic dipole moments. It will become clear, however, that simply by studying neutrino-electron scattering it is impossible to decide whether a nontrivial effect due to Eq. (3.1) is to be translated into an electric or magnetic neutrino dipole moment.

In the SM, a nonzero neutrino magnetic moment is generated at the one-loop level through the electroweak diagrams depicted in Fig. 2 and is given, in terms of the Bohr magneton $\mu_B = e/2m_e$, by [35]

$$\mu_\nu^{ij} \leq \frac{3eG_F}{8\sqrt{2}\pi^2} m_\nu = 3 \times 10^{-20} \mu_B \left(\frac{m_\nu}{10^{-1}\ \text{eV}}\right). \tag{3.2}$$

This is over 8 orders of magnitude below the sensitivity of foreseeable future probes of neutrino magnetic moments. For completeness, we mention that, also in the SM, neutrinos are expected to have a nonzero electric dipole moment, which is many, many orders of magnitude smaller

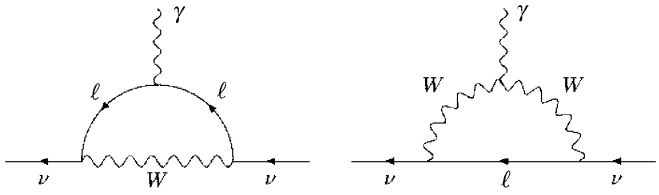

FIG. 2. Standard model one-loop contributions to the neutrino magnetic moment.

than the SM expectation for the neutrino magnetic dipole moment. Many manifestations of physics beyond the SM, however, predict much larger values for the neutrino magnetic moment [36]. The observation of a neutrino magnetic moment any time in the foreseeable future implies the existence of physics beyond the standard electroweak interactions.

The $i = j$ elements of μ_ν^{ij}, or *diagonal moments*, couple neutrinos of the same mass, while the ij elements, or *transition moments*, couple different mass eigenstates.[5] In the case of Majorana neutrinos, μ_ν^{ij} is constrained to be antisymmetric by *CPT* invariance; that is the requirement that the neutrino and antineutrino must have magnetic moments of equal magnitude. Thus, Majorana neutrinos possess only transition moments, whereas Dirac neutrinos can possess both diagonal and transition moments (this statement is weak-basis independent).

The presence of Eq. (3.1) modifies the neutrino-electron elastic scattering cross sections given by Eq. (2.2) in a dramatic way. The important point to realize is that the final state in this process contains a right-handed neutrino state; fundamentally distinguishable from the SM final state contribution. It must therefore be added incoherently to the SM event rate. Furthermore, a calculation of the total effect requires a sum over all possible final state neutrinos since they are unobserved. The net result is the additional term in the cross section [37]:

$$\frac{d\sigma}{dT}(\nu_j e \to \nu_i e)_{em} = \mu^2 \frac{\pi\alpha^2}{E_\nu m_e^2}\left(\frac{E_\nu}{T} - 1\right). \tag{3.3}$$

The signature of the magnetic moment effect is therefore an excess of events above the SM prediction displaying a characteristic T^{-1} dependence. Here, μ is now an effective dipole moment, generally given by $\mu_j^2 = \sum_i |\mu_\nu^{ij}|^2$, where the sum is performed over all possible final states. Of course, in the case of a short-baseline scattering experiment, the incoming neutrino is best represented by a flavor eigenstate, in which case it is most practical to constrain

[5]In this discussion we are assuming implicitly that the μ_ν^{ij} are expressed in the mass eigenbasis and define transition and diagonal moments using this convention. In the flavor basis, the magnetic moment matrix is transformed by the unitary neutrino mixing matrix U. In the Majorana case, for example, these would be related via $\mu^{\alpha\beta} = U\mu^{ij}U^T$.

$\mu_\alpha = \sum_\beta \mu^{\alpha\beta}$, α, $\beta = e$, μ, τ. Notice that this makes it impossible to determine the nature of the neutrino in such scattering experiments, as one cannot distinguish transition from diagonal moments. Matters are complicated further when dealing with sources composed of multiple neutrino flavors. In this case one experimentally extracts (or places an upper limit on) an effective moment, which is a weighted average of the moments of each beam flavor component: $\mu^2_{\rm eff} = \sum_\alpha \mu^2_\alpha f_\alpha$, where

$$\frac{df_\alpha(T)}{dT} = \frac{\int_T^\infty dE_\nu \frac{d\Phi_\alpha(E_\nu)}{dE_\nu}(\frac{E_\nu}{T} - 1)}{\sum_\beta \int_T^\infty dE_\nu \frac{d\Phi_\beta(E_\nu)}{dE_\nu}(\frac{E_\nu}{T} - 1)}. \tag{3.4}$$

$\mu_{\rm eff}$ traces out an ellipsoid in magnetic moment space. If an upper limit u is extracted on the effective moment, the strongest limit one can place on μ_α is $\mu_\alpha < u/\sqrt{f_\alpha}$. At a 50 GeV neutrino factory, $\mu_{\rm eff}$ is related to μ_α by $\mu^2_{\rm eff} \approx \frac{6}{11}\mu_e^2 + \frac{5}{11}\mu_\mu^2$. This relation was obtained by performing the necessary integrals and neglecting all terms except those proportional to $\ln T^{\rm min}/E_\nu^{\rm max}$. Notice that both moments contribute about equally, but a slightly tighter limit can be placed on μ_e as expected from the low energy behavior of the neutrino factory energy spectrum (see Fig. 1). With all of this in mind, it is clear that the experimentally measured magnetic moment is a very convoluted quantity, and therefore, one must take great care in interpreting/comparing such experimental results.

Currently, the tightest bounds on the neutrino magnetic moment come from astrophysics [38]. These limits arise from considerations of stellar/supernova cooling and are somewhat model dependent. Generally, such bounds are of order $(10^{-10}$–$10^{-12})\mu_B$, a far cry from the $10^{-19}\mu_B$ predicted from the minimally extended SM. Direct measurements via neutrino scattering are less model dependent, easier to interpret, and are quickly approaching a precision competitive with astrophysics.

Nuclear reactors offer an ideal setting for studying μ_e with $\bar\nu_e$ electron scattering due to the low energy peak of the neutrino spectrum (where magnetic moment effects are most prominent), and the ability to compare the on/off reactor states. Most recently, the MUNU [39] experiment at the Bugey reactor in France and TEXONO [40] at the Kuo-Sheng reactor in Taiwan have analyzed the recoil electron energy spectrum dN/dT for very small recoil kinetic energies, $T \lesssim 1$ MeV. The large uncertainties associated with the flux normalization at these energies were overcome by the potentially huge magnetic moment-induced excess that would either dwarf the SM background or allow the extraction of a strong upper bound. Their respective 90% confidence limits are $9 \times 10^{-11}\mu_B$ and $1.3 \times 10^{-10}\mu_B$. Our analysis, on the other hand, yields a 68% confidence level upper bound of $4.8 \times 10^{-10}\mu_B$ by considering the high energy tail of the spectrum, where the overall normalization is well known. μ_e is also accessible at beta-beam sources. A 68% upper bound of $3.0(6.6) \times 10^{-10}\mu_B$ and $2.6(6.7) \times 10^{-10}\mu_B$ is achievable at a ν_e, $\bar\nu_e$ β-beam source, respectively, assuming 0% (5%) systematic uncertainty. The authors of [41] also consider the determination of the electron neutrino magnetic moment at various sources including reactor and beta beams with similar results.

As for the other neutrino flavors: the LSND [42] experiment provides the best upper limit value of $6.8 \times 10^{-10}\mu_B$ on μ_μ. A future neutrino factory experiment could, at best, improve on this by a factor of 10. With a 0% (5%) assumed systematic uncertainty, a 50 GeV neutrino factory experiment can produce an upper bound on the effective magnetic moment of $2.5(10.1) \times 10^{-11}\mu_B$ and $3.1(12.4) \times 10^{-11}\mu_B$ at 68% confidence for a μ^+ and μ^- beam, respectively. The corresponding bounds on μ_e and μ_μ can be found by including the factors 1.35 and 1.48, respectively, as described above. For the NuMI beam, an upper limit on μ_μ of $1.8(6.6) \times 10^{-10}\mu_B$ can be achieved, and could be pushed below $10^{-10}\mu_B$ with a new/upgraded proton driver [27]. Thus far, we have said nothing about μ_τ. At the energies considered here ν_τ's cannot be produced, save for $\nu_\mu \to \nu_\tau$ oscillation effects which are negligible at our assumed short baseline of 100 m. Although our analysis cannot add to the subject, we point out, for completeness, that the Fermilab DONUT experiment has set a weak upper bound of $3.7 \times 10^{-7}\mu_B$ on μ_τ at 90% confidence [43].

C. Neutrino Z' couplings: ϵ

The existence of hypothetical heavy states that couple to both electrons and neutrinos would modify the differential cross section for neutrino-electron scattering. Such heavy states are ubiquitous in models of the physics that lies beyond the SM.

At center-of-mass energies well below the masses of the hypothetical heavy states, contributions to neutrino-electron scattering are very well captured by the introduction of effective four-fermion operators of the type $\bar\nu\Gamma\nu'\bar e\Gamma e$, where Γ stand for the various distinct combinations of Dirac gamma matrices, while ν and ν' stand for potentially distinct neutrino flavors. Here, we will concentrate on flavor independent vector-vector interactions, described by

$$\mathcal{L} = \epsilon(2\sqrt{2}G_\mu)\bar\nu_\ell\gamma^\alpha\nu_\ell\bar e\gamma_\alpha e + \text{H.c.}, \tag{3.5}$$

where ϵ is the new coupling constant, and refer to, for example, [44,45] for a more detailed study. While we appreciate the fact that this phenomenon is potentially much richer, for the purposes of our study, computing the sensitivity to ϵ, as defined in Eq. (3.5), will suffice in order to estimate the ability of future νe-scattering experiments to probe nonstandard neutrino interactions. On the other hand, the presence of a new, heavy neutral gauge boson (which we refer to, generically, as a Z') that couples universally to all three neutrinos and to right-handed and

left-handed electrons with equal strength would yield such an effective Lagrangian. Hence, we refer to ϵ as the neutrino-Z' coupling.

With the addition of Eq. (3.5), Eq. (2.2) still describes νe scattering, as long as one replaces

$$a \to a + \epsilon, \qquad b \to b + \epsilon. \tag{3.6}$$

At a reactor facility, we find that a 68% upper limit of 2×10^{-3} can be set on ϵ.[6] The limits set at a neutrino factory are potentially 1 order of magnitude better, $6.9(13.1) \times 10^{-4}$ and $3.3(8.7) \times 10^{-4}$ for a μ^+ and μ^- beam, respectively, assuming 0% (5%) systematic uncertainty. Our estimate for the neutrino factory agree with estimates obtained in [44]. At a beta-beam facility we find 68% upper bounds for ϵ of $9.8(16.3) \times 10^{-4}$ and $7.7(14.2) \times 10^{-4}$ for the ν_e and $\bar{\nu}_e$ modes, respectively. Finally, a conventional neutrino beam should set a bound of $2.7(6.4) \times 10^{-3}$. Other neutrino sources (including the sun) also allow one to probe for the existence of new neutrino-electron interactions, as recently discussed in [45].

D. Nature of the neutrino-Z-boson coupling: ρ

In the SM, the neutrino coupling to Z-bosons is purely left handed. In Sec. II, we defined the left-handed neutrino-Z-boson coupling as ρ, which is, in the SM, equal to unity at tree level. Its interesting to appreciate, however, that, experimentally, the left-handed nature of the neutrino coupling to the Z-boson is far from an established fact (for a detail discussion of this issue, see [47]).

The most precise information regarding the neutrino-Z-boson coupling is provided by precision studies of the invisible Z-boson width [31]. These, however, are not sensitive to the left-handed neutrino coupling to the Z-boson, but to a combination of the right-handed and the left-handed couplings to the Z-boson. More insight can only be obtained by combining Z-pole data with that obtained in neutrino scattering. The most robust bound on the left-handed-Z-boson coupling is obtained by combining Z-pole and CHARM-II data [48]. According to [47], ρ values as small as 0.9 are not ruled out (at around the three sigma level) as long as the right-handed neutrino-Z-boson coupling is nonzero (it is currently bound to be roughly less than 40% of the left-handed one [47]).

The main point is that, in neutrino-electron scattering, the incoming neutrino (antineutrino) beams are purely left handed (right handed). Hence, regardless of whether there are right-handed neutrino Z-boson couplings, the neutral current contribution to $\nu_\ell e \to \nu_\ell e$ is only dependent on ρ. For the strictly neutral current processes $\nu_\ell e \to \nu_\ell e$ and $\bar{\nu}_\ell e \to \bar{\nu}_\ell e$ ($\ell = \mu, \tau$), the cross section is proportional to ρ^2.[7] As only the total event rates are affected, it is expected that the capability of experiments with $\nu_\mu(\bar{\nu}_\mu)$ beams to constrain ρ should be limited. This is the condition of decay-in-flight conventional neutrino sources, where typically the electron neutrino beam component only contributes at the subpercent level. Currently, the most precise determination of ρ comes from the CHARM-II [48] collaboration at the CERN SPS conventional beam source. Their result, consistent with the SM prediction of $\rho = 1$, is precise to $\delta\rho = 3.4\%$. In our analysis, assuming the NuMI beam, we conclude that ρ can be measured to only 3.3% (7.3%) assuming 0% (5%) systematic uncertainty; clearly comparable to the CHARM-II result. Most of the uncertainty is related to the rather poor knowledge of the overall normalization of the neutrino flux.

Reactions with $\nu_e(\bar{\nu}_e)$ involve both charged and neutral current terms, and the interference between them induces nontrivial changes to the recoil energy spectrum $dN_{\rm SM}(T)/dT$ described by Eq. (2.1). Allowing for arbitrary ρ values, the a, b parameters of Eq. (2.2) read

$$\left.\begin{aligned} a &= \rho(\tfrac{1}{2} - \sin^2\theta_W) - 1 \\ b &= \rho(-\sin^2\theta_W) \end{aligned}\right\} \qquad \nu_e e \to \nu_e e. \tag{3.7}$$

Again, $a \leftrightarrow b$ for the $\bar{\nu}_e$ process. For this reason, measurements of $\nu_e - e$ scattering (or $\bar{\nu}_e - e$) are sensitive to ρ (and not ρ^2). Furthermore, not only is the total event rate modified, but so is the energy distribution of the recoil electrons. Finally, $\nu_e - e$ scattering is also sensitive to the *sign* of ρ, i.e., it depends on whether the W-boson exchange interferes destructively or constructively with the Z-boson exchange contribution [49]. In the SM ρ is positive—the Z-boson and W-boson exchange diagrams interfere destructively.

Several of the experimental setups considered here can extract (sometimes with high confidence) the sign of ρ. Indeed, such a feat has already been accomplished by early experiments sensitive to $\nu_e - e$ elastic scattering [50]. They find agreement with destructive interference ($\rho > 0$) at around the five sigma level. The reactor neutrino experimental setup considered here should be able to repeat such a sign determination using electron antineutrinos (which has not been accomplished yet), as long as it can accumulate enough statistics and control the uncertainty on the normalization of the $\bar{\nu}_e$ flux. We find, for example, that the future reactor experiments listed in [19] could easily determine the sign of ρ within one year of data collection, provided that systematic uncertainties (including flux normalization) are held below (25–30)%. Needless to say, β-beams should provide the ultimate tool when it comes to studying this issue in detail.

When setting bounds on ρ, we explicitly assume that it is positive. Our estimates are summarized in Table III. We

[6] A detailed study of the electron g_L and g_R couplings using reactor data was performed in [46]. Bounds on g_L and g_R can be easily converted into bounds on ϵ (among other possibilities).

[7] For simplicity, we assume that ρ is flavor independent.

find that a future reactor experiment should measure ρ to 1.1%. At a beta-beam source, this can be reduced to 0.39% (2.4%) and 0.75% (3.1%) for a ν_e and $\bar{\nu}_e$ beam, respectively, assuming 0% (5%) systematic uncertainty. At a neutrino factory, assuming the same range of systematic uncertainties, we expect a precision of 0.09% (1.2%) and 0.06% (0.93%) for a μ^+ and μ^- beam, respectively. As mentioned earlier, we have assumed that the value of ρ is flavor universal, so that, in the case of a neutrino factory, information is obtained from both the ν_μ and the ν_e components of the beam.

IV. CONCLUDING REMARKS

Neutrino-electron scattering provides a very clean environment for detailed studies of electroweak interactions. In principle, one is not only capable of precisely determining the value of SM parameters, but is also sensitive to physics beyond the SM, including anomalous neutrino couplings to photons, neutrino and electron couplings to new neutral gauge bosons (Z primes), and right-handed neutrino neutral currents.

On the negative side, the cross section for neutrino-electron scattering is tiny. This means that one needs very large neutrino sources and/or neutrino targets. Moreover, backgrounds related to neutrino-nucleon scattering, whose cross section is around 3 orders of magnitude larger, need to be seriously suppressed. Finally, competitive precision measurements can only be performed if the neutrino beams are very well understood (shape and normalization).

It is now clear that, in the foreseeable future, new neutrino facilities, where the obstacles summarized above can be eliminated, will become available. The new physics revealed by neutrino oscillation experiments calls for very intense, very well understood neutrino sources, and these are currently under serious consideration. Furthermore, many of these planned facilities will house ''near detectors,'' for several reasons. The types of setups we are considering qualify as near detectors (not unlike the Minerva experiment, currently being planned as a new detector to be added to the MINOS near detector).

Here, we have estimated how precisely various observables could be measured via neutrino-electron elastic scattering at existing (say, the NuMI beam) and future facilities, including neutrino factories, β-beams, and next-generation, large detectors located close to powerful nuclear reactors. Table III summarizes our results, as well as the assumptions that went into extracting them. For most setups, we have quoted expectations in the case that systematic uncertainties are reduced to negligible levels—results with relatively large systematic uncertainties are quoted in Sec. III. Ultimately, the ''correct'' estimate for systematic effects will be obtained by the experimental collaborations. We believe, however, that our estimates can be considered representative of either a typical or a worst-case scenario.

In summary, it is fair to say that, in the foreseeable future, we can expect neutrino-electron scattering experiments to contribute, in a significant way, to our understanding of electroweak interactions—and beyond. We urge experimentalists to keep the possibility of performing precision neutrino-electron scattering studies when developing next-generation ''near detectors'' for future neutrino facilities.

ACKNOWLEDGMENTS

We thank Olga Mena for very useful conversations, for information regarding the neutrino fluxes from different future neutrino facilities, and for comments on the manuscript. We are also indebted to Boris Kayser for fruitful conversations on the neutrino coupling to the Z-boson. This work is sponsored in part by the U.S. Department of Energy Contract No. DE-FG02-91ER40684.

[1] C. Albright *et al.* (Neutrino Factory/Muon Collider Collaboration), physics/0411123.
[2] D. Drakoulakos *et al.* (Minerva Collaboration), hep-ex/0405002.
[3] S. Eidelman *et al.* (Particle Data Group Collaboration), Phys. Lett. B **592**, 1 (2004).
[4] J. N. Bahcall, M. Kamionkowski, and A. Sirlin, Phys. Rev. D **51**, 6146 (1995).
[5] W. J. Marciano and A. Sirlin, Phys. Rev. D **22**, 2695 (1980); **31**, 213(E) (1985).
[6] S. Sarantakos, A. Sirlin, and W. J. Marciano, Nucl. Phys. **B217**, 84 (1983).
[7] M. Drees, DESY Report No. DESY-91-045.
[8] W. J. Marciano and Z. Parsa, J. Phys. G **29**, 2629 (2003); see also M. Passera, Phys. Rev. D **64**, 113002 (2001).
[9] See, for example, R. Imlay and G. J. VanDalen, J. Phys. G **29**, 2647 (2003).
[10] C. Bemporad, G. Gratta, and P. Vogel, Rev. Mod. Phys. **74**, 297 (2002).
[11] H. B. Li and H. T. Wong, J. Phys. G **28**, 1453 (2002).
[12] P. Vogel and J. Engel, Phys. Rev. D **39**, 3378 (1989).
[13] H. Murayama and A. Pierce, Phys. Rev. D **65**, 013012 (2001).
[14] P. Huber and T. Schwetz, Phys. Rev. D **70**, 053011 (2004).
[15] For recent studies related to observing this process, see, for example, H. T. Wong, H. B. Li, J. Li, Q. Yue, and Z. Y. Zhou, J. Phys.: Conf. Ser. **39**, 266 (2006).

[16] J. M. Conrad, J. M. Link, and M. H. Shaevitz, Phys. Rev. D **71**, 073013 (2005).
[17] M. Apollonio *et al.* (CHOOZ Collaboration), Phys. Lett. B **420**, 397 (1998).
[18] K. Anderson *et al.*, hep-ex/0402041.
[19] M. Goodman, Nucl. Phys. B, Proc. Suppl. **145**, 186 (2005).
[20] F. Ardellier *et al.*, hep-ex/0405032.
[21] S. Geer, Phys. Rev. D **57**, 6989 (1998); **59**, 039903(E) (1999).
[22] M. L. Mangano *et al.*, hep-ph/0105155.
[23] J. Burguet-Castell, D. Casper, J. J. Gomez-Cadenas, P. Hernandez, and F. Sanchez, Nucl. Phys. **B695**, 217 (2004).
[24] S. H. Ahn *et al.* (K2K Collaboration), Phys. Lett. B **511**, 178 (2001).
[25] For a recent discussion of the current status of T2K, see Y. Oyama, hep-ex/0512041.
[26] L. Bugel *et al.* (FINeSSE Collaboration), hep-ex/0402007.
[27] M. G. Albrow *et al.*, hep-ex/0509019.
[28] Olga Mena (private communication).
[29] G. P. Zeller *et al.* (NuTeV Collaboration), Phys. Rev. Lett. **88**, 091802 (2002); **90**, 239902(E) (2003).
[30] S. Davidson, S. Forte, P. Gambino, N. Rius, and A. Strumia, J. High Energy Phys. 02 (2002) 037.
[31] S. Schael *et al.*, Phys. Rep. **427**, 257 (2006).
[32] D. Geiregat *et al.* (CHARM-II Collaboration), Phys. Lett. B **259**, 499 (1991); P. Vilain *et al.* (CHARM-II Collaboration), Phys. Lett. B **281**, 159 (1992).
[33] L. A. Ahrens *et al.*, Phys. Rev. D **41**, 3297 (1990).
[34] A. B. Balantekin, J. H. de Jesus, and C. Volpe, Phys. Lett. B **634**, 180 (2006).
[35] K. Fujikawa and R. Shrock, Phys. Rev. Lett. **45**, 963 (1980).
[36] For recent reviews, see, for example, R. N. Mohapatra *et al.*, hep-ph/0510213; A. de Gouvêa, Nucl. Phys. B, Proc. Suppl. **143**, 167 (2005).
[37] A. V. Kyuldjiev, Nucl. Phys. **B243**, 387 (1984).
[38] H. T. Wong and H. B. Li, Mod. Phys. Lett. A **20**, 1103 (2005).
[39] Z. Daraktchieva *et al.* (MUNU Collaboration), Phys. Lett. B **615**, 153 (2005).
[40] H. B. Li *et al.* (TEXONO Collaboration), Phys. Rev. Lett. **90**, 131802 (2003).
[41] G. C. McLaughlin and C. Volpe, Phys. Lett. B **591**, 229 (2004).
[42] L. B. Auerbach *et al.* (LSND Collaboration), Phys. Rev. D **63**, 112001 (2001).
[43] R. Schwienhorst *et al.* (DONUT Collaboration), Phys. Lett. B **513**, 23 (2001).
[44] S. Davidson, C. Peña-Garay, N. Rius, and A. Santamaria, J. High Energy Phys. 03 (2003) 011.
[45] J. Barranco, O. G. Miranda, C. A. Moura, and J. W. F. Valle, Phys. Rev. D **73**, 113001 (2006).
[46] J. L. Rosner, Phys. Rev. D **70**, 037301 (2004).
[47] M. Carena, A. de Gouvêa, A. Freitas, and M. Schmitt, Phys. Rev. D **68**, 113007 (2003).
[48] P. Vilain *et al.* (CHARM-II Collaboration), Phys. Lett. B **320**, 203 (1994).
[49] B. Kayser, E. Fischbach, S. P. Rosen, and H. Spivack, Phys. Rev. D **20**, 87 (1979).
[50] R. C. Allen *et al.*, Phys. Rev. Lett. **64**, 1330 (1990); L. B. Auerbach *et al.* (LSND Collaboration), Phys. Rev. D **63**, 112001 (2001).